PROFILE DISPERSION MEASUREMENTS FOR OPTICAL FIBRES OVER THE WAVELENGTH RANGE 350nm to 1900nm

F.M.E.Sladen, D.N.Payne and M.J.Adams
Department of Electronics, University of Southampton
Southampton SO9 5NH, England.

Pulse spreading in multimode optical fibres is caused primarily by a) transit-time differences which exist between modes and b) material dispersion effects which are apparent when using non-monochromatic sources. The resultant pulse spreading may be minimised, respectively, by designing graded-core fibres with optimal refractive-index profiles, and by operating in the wavelength range 1.27-1.35μm, where the material dispersion effect is small [1]. In order to optimise refractive-index profiles in this longer-wavelength region it is essential to possess accurate refractive-index data on commonly-used fibre materials over a wider spectral range than has been hitherto available. In this paper we present for the first time results giving the required optimum index profile over the extended wavelength range 350nm to 1900nm, thus allowing fibre design for the 1.3μm region. Furthermore, the expansion which has been achieved in the wavelength range of the measurements has resulted in a considerable improvement in accuracy over the results reported previously [2].

In the case of silica fibres doped with germania, phosphorous or boron, a large amount of data is now available, albeit over a restricted wavelength range, concerning the dispersive properties of the materials. The data has been obtained on fibres [2,3] and on bulk glasses [4,5,6] and should serve to aid the design of fibres with minimal pulse spreading. Unfortunately, however, considerable discrepancies appear to exist between data reported from different sources, leading to confusion as regards the optimum index profile for a given wavelength of operation. These discrepancies are that a) both fibre and bulk-glass results differ between samples having different compositions and (b) bulk-glass results differ from those found in fibres. Two suggestions have emerged to explain these inconsistencies. Firstly, it is argued that the glasses exhibit inhomogeneous dispersion, i.e. that the dispersive properties of the materials are not linearly related to their composition, leading to results which differ according to the particular sample composition. Secondly, it is thought that the wavelength-dispersive properties of the glasses are affected by the thermal histories of the samples and thus an annealed bulk sample yields results different from those obtained from a fibre, the latter having experienced severe chilling during drawing.

The improved accuracy which has resulted from the extended wavelength range of the measurements has enabled us to test the above-noted hypotheses for germania-doped glasses. Firstly, the wavelength dispersive properties as a function of composition may be determined by measuring a range of step-index fibres having different germania concentrations. Secondly, by measuring a fibre sample annealed so as to simulate the cooling of a bulk glass sample it is possible to discover the differences which exist in dispersive properties as a result of thermal history.

Theory

Olshansky and Keck [7] considered pulse broadening due to inter-modal delay differences in the class of fibres with α-law profiles and predicted the optimum profile which maximises the bandwidth as

$$\alpha_{opt} = 2 - 2P - 12\Delta/5 \qquad \ldots (1)$$

where Δ is the relative index difference between core centre and cladding and P is the profile dispersion parameter defined as

$$P = \frac{n_1}{N_1} \frac{\lambda}{\Delta} \frac{d\Delta}{d\lambda} \qquad \ldots (2)$$

Here n_1 is the index at core centre, λ is the operating wavelength and $N_1 = n_1 - \lambda dn_1/d\lambda$ is the group index. Implicit in this theory is the assumption that the parameter P is a constant throughout the core, i.e. that P is independent of material composition. This may be restated as a requirement that $dn/d\lambda$ varies linearly with the index n for all compositions. Such a relationship would result if, for example, it were found that over a range of wavelengths the refractive index of a binary silica/germania glass varied linearly with germania content. This would not appear unlikely in view of the relatively low dopant levels used.

If on the other hand the profile dispersion is found to be a continuous function of core radius in a graded-index fibre, then other more complex and conceptually less-appealing analyses are required [8] and the optimum profile is no longer of the power-law type. A further possibility which has been recently analysed [9,10] is that two or more dopants may be incorporated in the core, the doping profile being different for each component. In this case, the profile dispersion is clearly not a constant within the core; however, if the assumption may be made that the profile dispersion for each component is independent of its concentration, considerable simplification of the analysis results and it may even be possible by appropriate choice of doping profiles to design waveguides having optimal properties over a broad wavelength range [10]. Thus it is crucial that a knowledge of the behaviour of the profile dispersion as a function of dopant concentration is obtained, particularly since earlier results [4] show that major variations exist which would preclude the above-noted simplified analysis.

Experiment

Details of our experimental technique for the measurement of P directly on the fibre have already been reported [2]. Expansion of the range of the measurement further into the infra-red to 1900nm has been achieved by using a germanium as well as a silicon PIN photodetector, in conjunction with a prism monochromator for wavelength selection. In addition, further attention to experimental detail has considerably improved the accuracy and reproducibility of the method.

The raw data in the form of the variation of the fibre numerical aperture (na) with wavelength over the range 350nm to 1900nm is processed by a method developed in reference [2]. Using a least-squares technique the experimental data is fitted to an expanded Sellmeier equation of the form

$$(na)^2 = \Psi = a\lambda^2 + b/\lambda^2 + c \qquad \ldots (3)$$

Having determined the coefficients a, b and c of the fitted curve, the parameter P and hence α_{opt} may be computed, using eqns(1) and (2).

In order to obtain a realistic estimate of the certainty with which α_{opt} is determined by the experiment, an error analysis has been implemented on the set of data points $\Psi(\lambda)$ representing the variation of the square of the numerical aperture with wavelength. The

variance of Ψ can be found as

$$\text{var}(\Psi) = A\lambda^4 + B/\lambda^4 + C + D\lambda^2 + E/\lambda^2 + F \quad \ldots (4)$$

where A = var(a), B = var(b), C = var(c), D = 2cov(a,c), E = 2cov(b,c), F = 2cov(a,b). These variances and covariances of the coefficients are readily calculated at the same time as the least-squares determination of a,b and c.

Defining $\phi = 2(a\lambda^2 - b/\lambda^2)$ ... (5)

we find from (2) and (3) that

$$P \simeq \frac{n_1}{N_1}\frac{\lambda}{\Psi}\frac{d\Psi}{d\lambda} = \frac{n_1}{N_1}\frac{\phi}{\Psi} \quad \ldots (6)$$

The variance of P is then given by

$$\text{var}(P) = \frac{n_1}{N_1}\text{var}\left(\frac{\phi}{\Psi}\right) \simeq \left[\frac{n_1}{N_1}\right]^2\left[\frac{\text{var}\phi}{\Psi^2} + \frac{\phi^2}{\Psi^4}\text{var}(\Psi)\right] \quad \ldots (7)$$

where higher order terms on the r.h.s. of (7) are usually negligible. In order to evaluate this expression we require var(ϕ) which, from (5), is

$$\text{var}(\phi) = 4(A\lambda^4 + B/\lambda^4 - F) \quad \ldots (8)$$

Equations (5), (7) and (8) permit a simple evaluation of the variance of the deduced value of P, and hence of α_{opt} as a function of wavelength. As expected, we find that the variance of α_{opt} increases rapidly towards the extremities of the 350 to 1900nm measurement range and indicates moreover that attempting to extrapolate outside of the range would be unwise. The analysis reveals that the predicted value for α_{opt} is most accurate over the wavelength range 700-1500nm, a typical error being ± 0.02.

Results

Measurements have been performed on B_2O_3 and P_2O_5-doped step-index fibres, together with a range of GeO_2-doped step-index fibres. The fibre characteristics are given in Table 1. The maximum GeO_2 content tested (13.1m/o) is typical of the level used at the core centre of graded-index fibres manufactured by the CVD process. Thus the three GeO_2 fibre samples enable a test to be made of the variation of the profile parameter P at three dopant levels commonly found within the core of a graded-index fibre.

Fibre Sample	Dopant	Concentration m/o
A	P_2O_5	12.0
B	B_2O_3	10.0
C	GeO_2	8.1
D	GeO_2	11.0
E	GeO_2	13.1
F	GeO_2 annealed	8.1

Table 1

In order to test the effect of thermal history on the fibre samples the 8.1m/o GeO_2-doped fibre was subjected to an annealing schedule of 30 mins at 1230°C, followed by a gradual cooling to room temperature over a period of several hours. Although the thermal history of the bulk glass samples used in references [4-6] is not given, it is thought that the above schedule represents an adequate simulation.

The measured values of $(na)^2$ for the three dopant materials (samples A, B and D) together with the least squares fit using eqn (3) are given

in figs.(1a),(2a) and (3a).It should be noted that the variation of numerical aperture is extremely small, particularly in the case of phosphosilicate glass and that, consequently, great care must be taken to ensure experimental accuracy. The variation of α_{opt} with wavelength deduced from the experimental data is illustrated in figs.(1b) (2b) and (3b) and we see that for both GeO_2-and B_2O_3-doped fibres α_{opt} changes considerably with wavelength, whilst for P_2O_5-doped fibres little variation exists over a wide wavelength range. Also shown on the figures are the computed 99% confidence limits obtained from the data using the error analysis outlined earlier. Note that such an analysis gives no indication of the extent of any systematic error; however, numerous experiments using different fibre samples and changing the experimental parameters indicate that this is of a similar order to the statistical error.

For completeness, the value of α_{opt} for all three materials is replotted in fig.4. In addition, the figure gives the results obtained on the three samples C, D and E having different GeO_2 concentrations. The curves are very nearly identical, being within the thickness of the line, clearly indicating that for the range of compositions tested α_{opt} is independent of concentration. This result differs considerably from those reported on bulk glasses [4,5,6] and leads us to believe that at least for germania-doped graded-index fibres profile dispersion is homogeneous throughout the core. We note also that our results for P_2O_5- and B_2O_3-doped glasses differ somewhat from earlier published results [3].

The effect of heat treatment on the wavelength-dispersive properties of a GeO_2-doped glass is illustrated in fig.5. The value of α_{opt} found for sample F is seen to be very similar to that obtained on the as-drawn fibre (sample C), a slight drop in α_{opt} being all that is evident. Since this reduction is of similar magnitude to the confidence limits computed for the untreated fibre, it is not at present clear whether even this small change is experimentally significant. We conclude, therefore, that the difference in thermal histories between samples of germania-doped glasses is insufficient to explain the presently-observed differences in profile dispersion measured on fibres and bulk glasses.

Implications for Fibre Systems

The choice of dopant material has a profound effect on fibre bandwidth if we consider the possibility of up-dating a system optimised for operation at 850nm to work in the 1.3μm window region where the material dispersion is negligibly small. Whereas a move to longer wavelength is accompanied by a reduction in the intra-modal dispersion caused by material dispersion, this will be offset to some degree by the increase in intermodal delay differences as the profile becomes non-optimal. The effect is shown in fig.(6a) and (b) where the Bit Rate x Length product is calculated as a function of operating wavelength from the theory of reference [7]. Using the values for α_{opt} given earlier, the curves are plotted for P_2O_5 and GeO_2-doped fibres which have been designed to operate at 850nm. Fig.(6a) gives the curves for a laser of 2nm spectral spread while (6b) gives the equivalent for an LED of 40nm. We see that in the case of the laser operating in conjunction with a germania-doped fibre the bandwidth actually decreases as we move to longer wavelength, while for P_2O_5-doped fibres with their characteristically low wavelength-variation of α_{opt}, we obtain the expected bandwidth improvement. The effect is equally marked for LED operation where for the GeO_2-doped fibre very

little improvement in bandwidth is gained by moving the operating wavelength to the 1.3μm region. In contrast, the P_2O_5-doped fibre exhibits an increase of nearly two orders of magnitude.

Conclusions

Improvements in the direct method for the measurement of the profile dispersion parameter P have enabled a major extension of the wavelength range, allowing the 1.3μm region to be covered. An accompanying improvement in accuracy has permitted for the first time a comparison of the values of P measured on fibres having different dopant concentrations, together with a determination of the effect of thermal history on the wavelength-dispersive properties of the glass. From our results it would appear that the profile dispersion is not dependent on the dopant concentration, at least for GeO_2-doped fibres having concentrations in the range measured. In addition, we find that the thermal history of a GeO_2-doped fibre has only a small effect on the measured value of P, thus eliminating the effect as the reason for observed differences between measurements on fibres and bulk-glass samples.

The profile dispersion results have been used to predict the bandwidth of fibres designed for operation at 850nm when subsequently employed at other wavelengths. The calculations indicate that in the case of germania-doped fibres excited by a laser diode a reduction in bandwidth occurs and thus uprating of such a fibre to 1.3μm operation would be of no advantage. Exploitation of the longer wavelength region therefore requires either the design of fibres specifically for 1.3μm operation, or the development of fibres which exhibit low pulse dispersion over an extended spectral range [10].

References

[1] D.N. Payne and A.H. Hartog, Electronics Letters, 1977, 13, 627-9.
[2] F.M.E. Sladen, D.N. Payne and M.J. Adams, Electronics Letters, 1977 13, 212-3.
[3] H.M. Presby and I.P. Kaminow, Appl. Optics 1976, 12, 3029-3036.
[4] J.W. Fleming, J.Am.Ceram.Soc. 1976, 59, 503-7.
[5] J.W. Fleming, Electronics Letters 1978, 14, 326-8.
[6] S. Kobayashi, S. Shibata, N. Shibata and T. Izawa, International Conference on Integrated Optics and Optical Fibre Communication 1977, Technical Digest, 309-312.
[7] R.Olshansky and D.B. Keck, Appl. Optics 1976, 15, 483-491.
[8] J.A. Arnaud, Opt. and Quantum Electron. 1977, 9, 111-119.
[9] E.A.J. Marcatili, B.S.T.J. 1977, 56, 49-63.
[10] R. Olshansky, Electronics Letters, 1978, 14, 330-331.

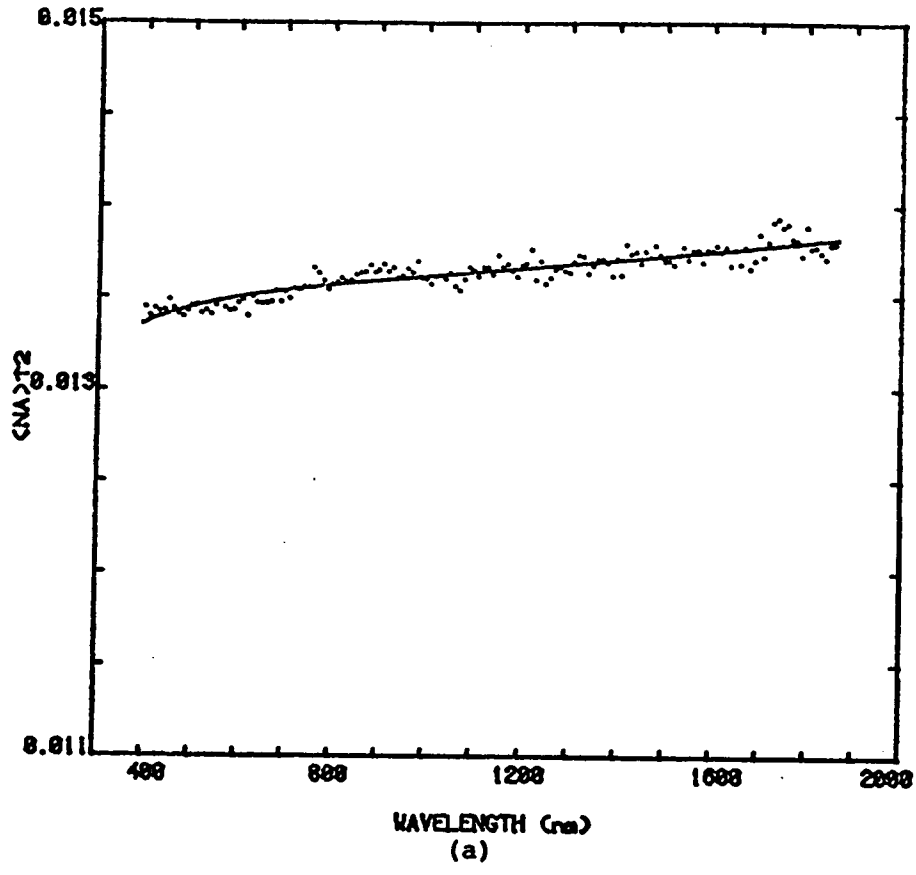

(a)

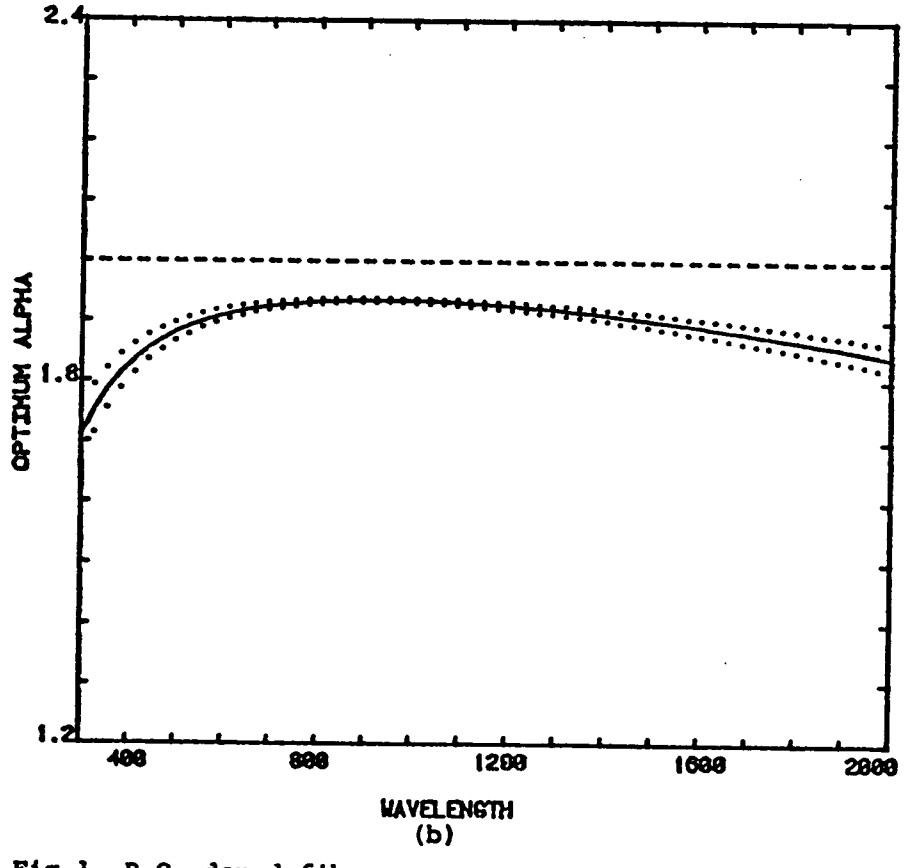

(b)

Fig.1 P_2O_5-doped fibres

(a) Variation of $(na)^2$ for a step-index fibre having a silica cladding (sample A)

(b) Optimum profile as a function of wavelength Dotted lines show certainty limits

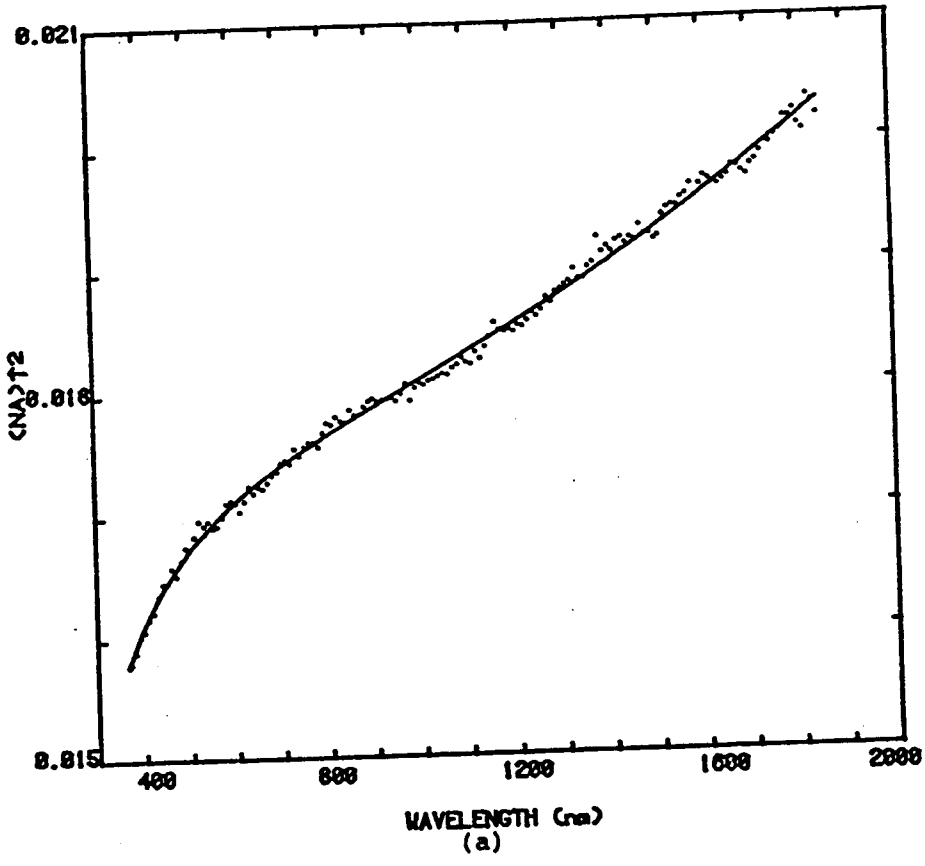

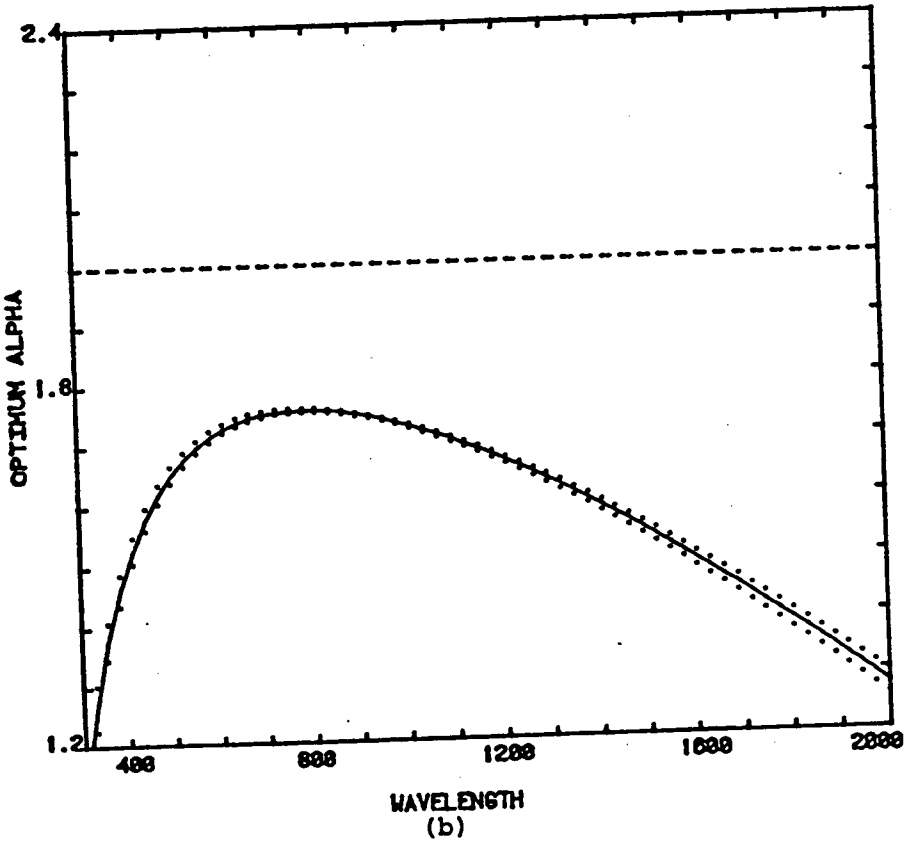

Fig.2 B_2O_3-doped fibres
(a) Variation of $(na)^2$ for a step-index fibre having a silica core (sample B)
(b) Optimum profile as a function of wavelength Dotted lines show certainty limits

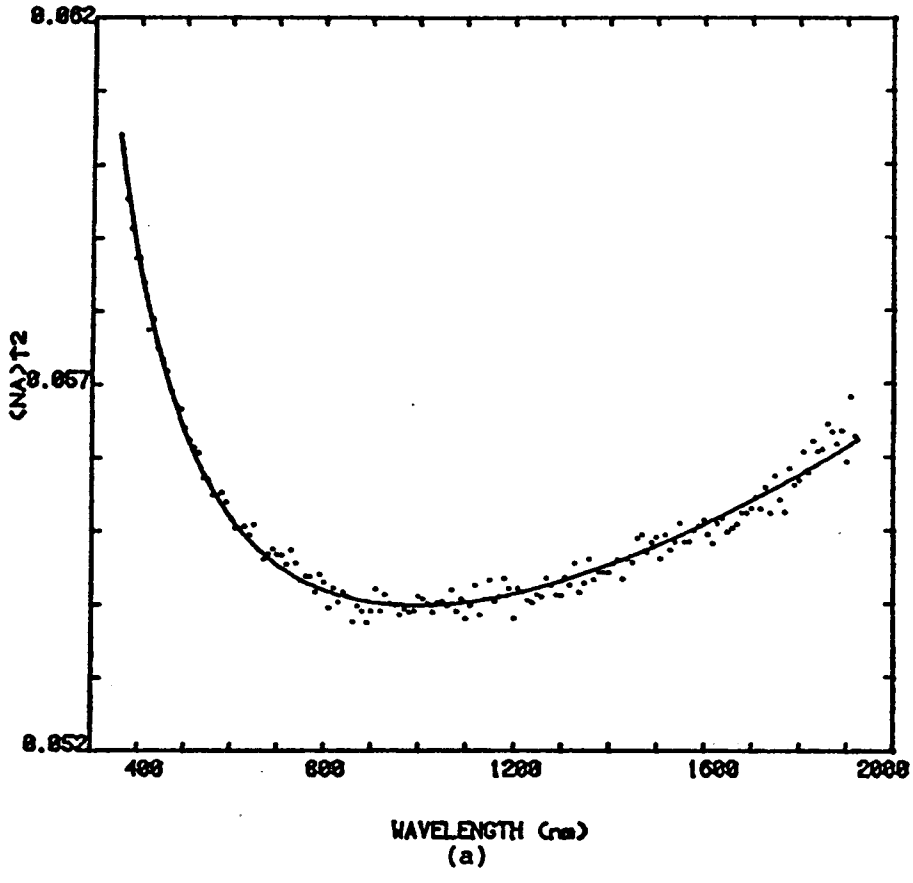

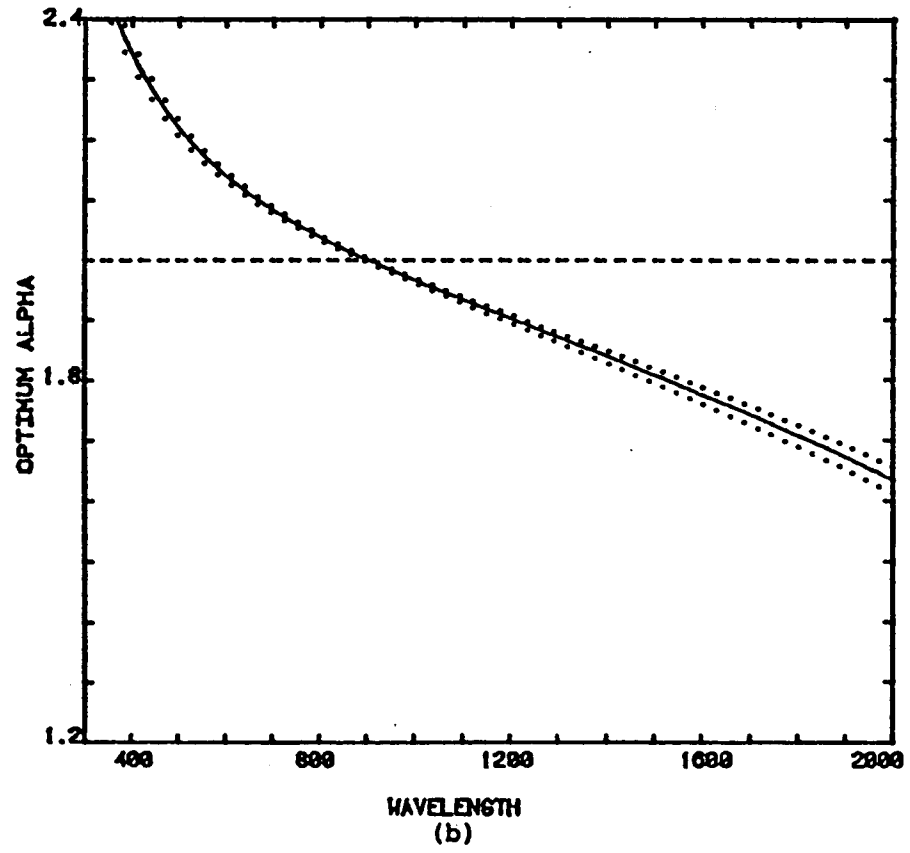

Fig.3 GeO_2-doped fibres

(a) Variation of $(na)^2$ for a step-index fibre having a silica cladding (sample D)

(b) Optimum profile as a function of wavelength Dotted lines show certainty limits

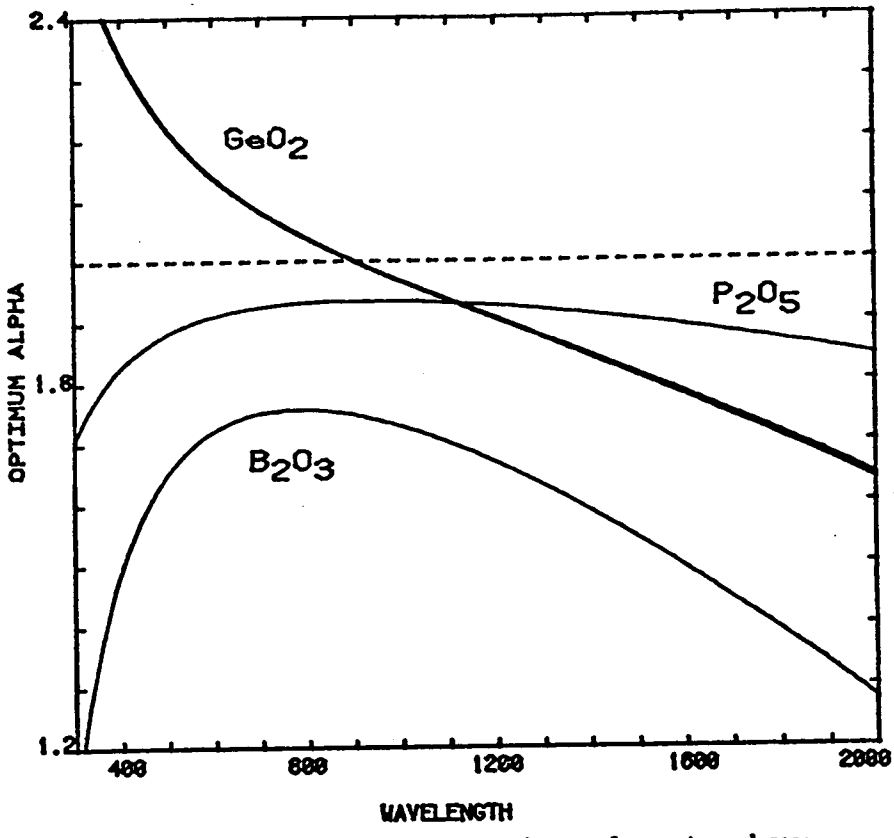

Fig.4 Optimum profile for the three dopants shown
The GeO_2 curve comprises results for three GeO_2 concentrations (samples C, D, E) which all lie within the thickness of a line

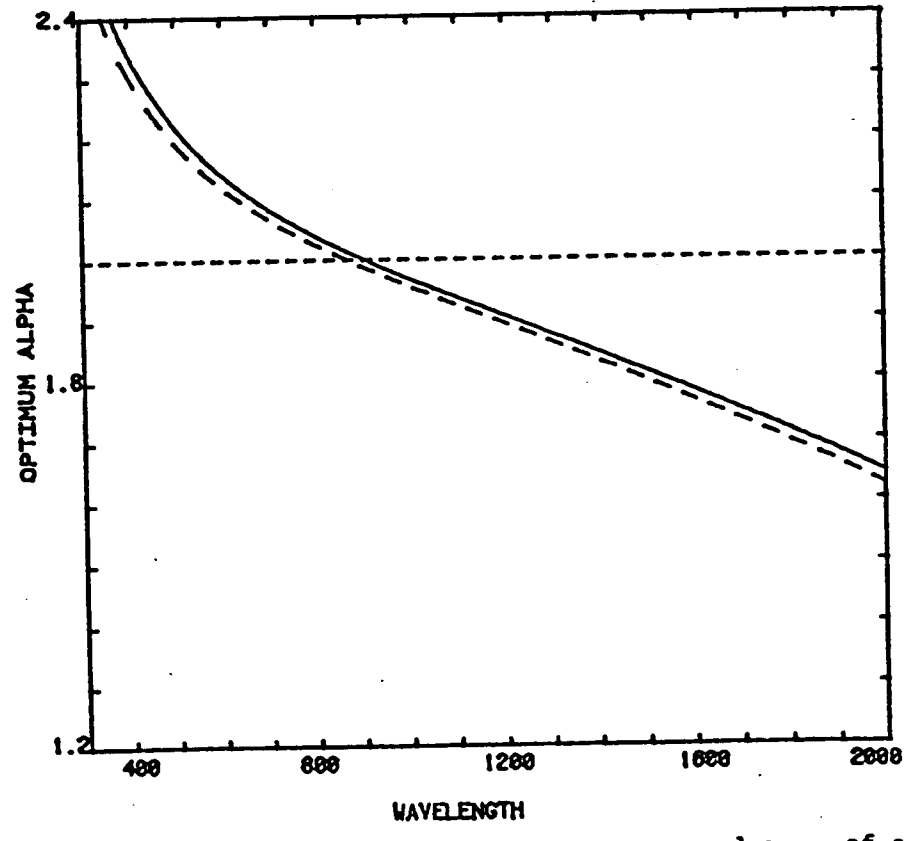

Fig. 5 Effect of thermal history on measured α_{opt} of a GeO_2-doped fibre
Solid line: As-drawn fibre (sample D)
Dotted line: Annealed fibre (sample F)

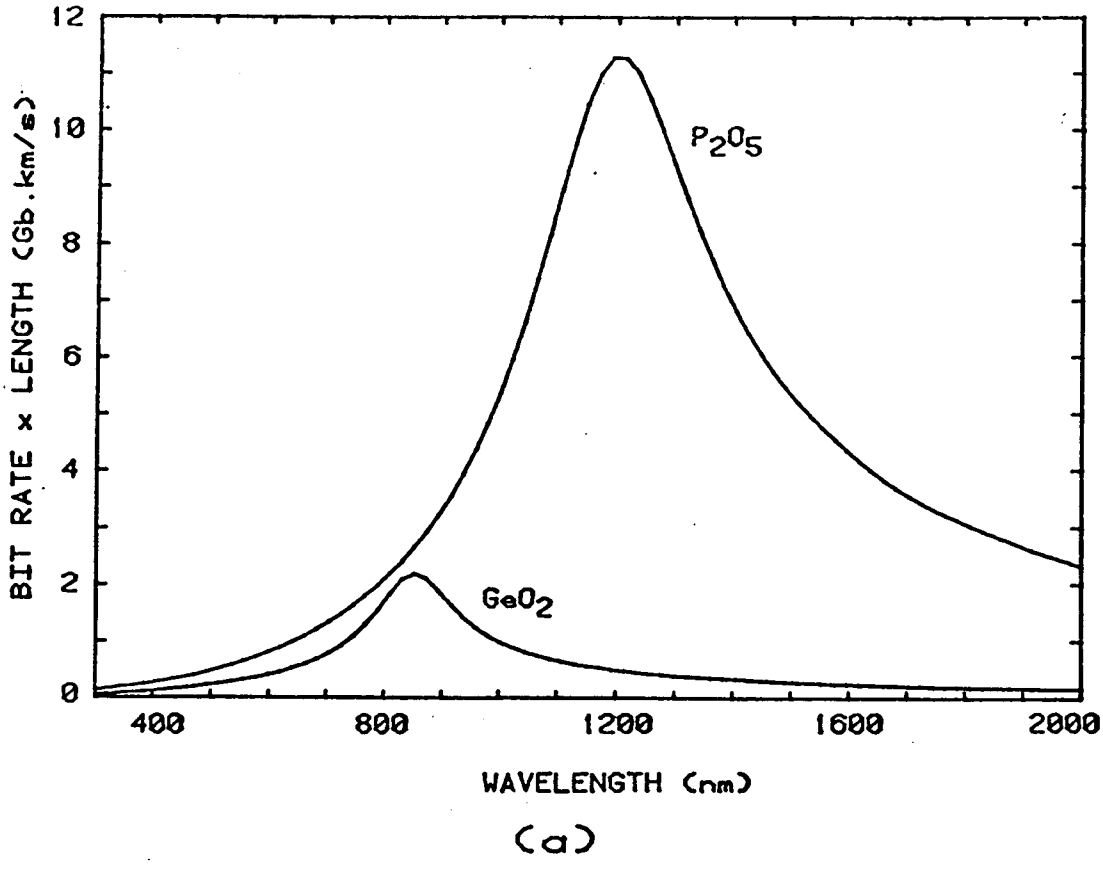

(a)

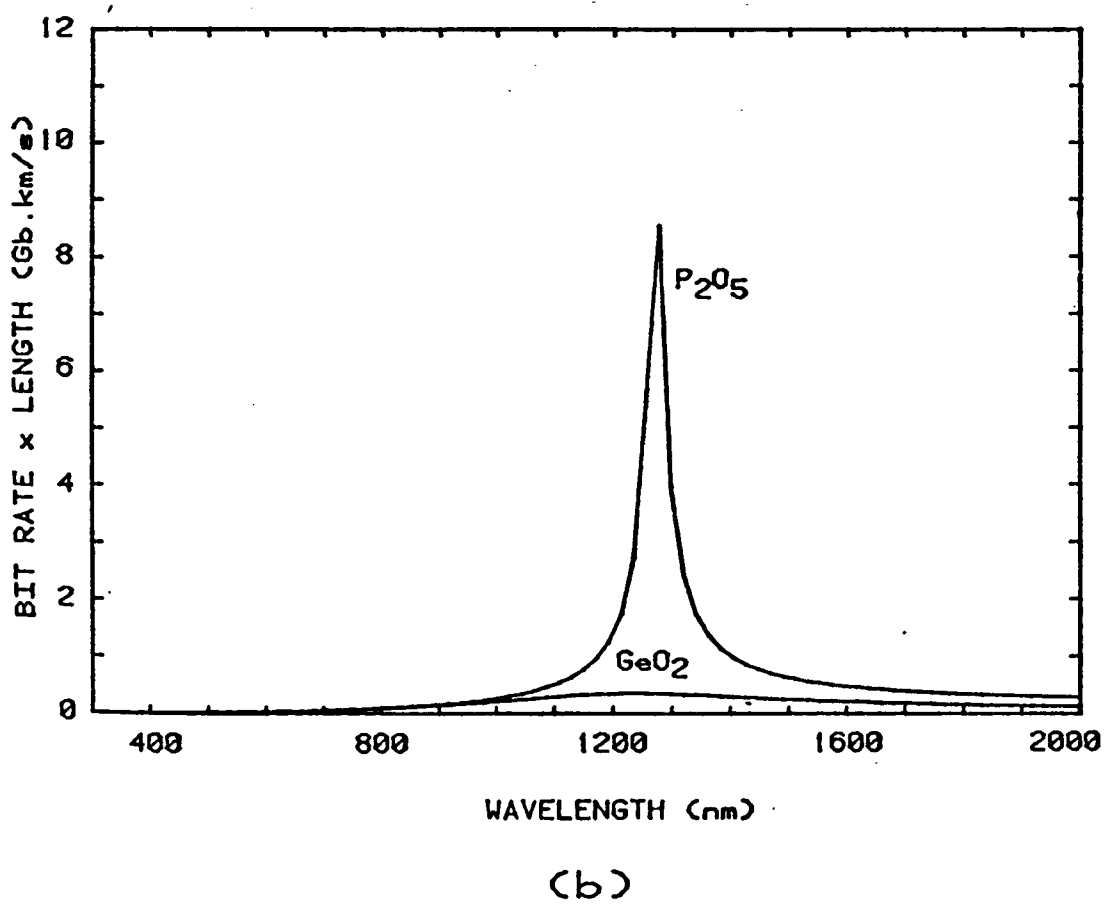

(b)

Fig.6 Variation of bandwidth with wavelength for fibres having a profile designed for operation at 850nm. The curves are plotted for fibres having P_2O_5 and GeO_2 content at core centre of 12 m/o and 13.1 m/o respectively.
(a) gives the result for a laser of 2nm spectral spread,
(b) that for an LED of 40nm